JMEPEG (2005) 14:249-257
DOI: 10.1361/10599490522365

1059-9495/$19.00

Effects of Electroplated Zinc-Nickel Alloy Coatings on the Fatigue Strength of AISI 4340 High-Strength Steel

H.J.C. Voorwald, I.M. Miguel, M.P. Peres, and M.O.H. Cioffi

(Submitted April 1, 2004)

Recovered substrates have been extensively used in the aerospace field. Cadmium electroplating has been widely applied to promote protective coatings in aeronautical components, resulting in excellent corrosion protection combined with a good performance in cyclic loading. Ecological considerations allied to the increasing demands for corrosion resistance have resulted in the search for possible alternatives. Zinc-nickel (Zn-Ni) alloys have received considerable interest recently, because these coatings show advantages such as a good resistance to white and red rust, high plating rates, and acceptance in the market. In this study, the effect of electroplated Zn-Ni coatings on AISI 4340 high-strength steel was analyzed for rotating bending fatigue strength, corrosion, and adhesion resistance. The compressive residual stress field was measured by x-ray diffraction prior to fatigue tests. Optical microscopy documented coating thickness, adhesion characteristics, and coverage extent for nearly all substrates. Fractured fatigue specimens were investigated using scanning electron microscopy (SEM). Three different Zn-Ni coating thicknesses were tested, and comparisons with the rotating bending fatigue data from electroplated Cd specimens were performed. Experimental results differentiated the effects of the various coatings on the AISI 4340 steel behavior when submitted to fatigue testing and the influence of coating thickness on the fatigue strength.

Keywords cadmium electroplating, corrosion, fatigue, zinc-nickel coatings

1. Introduction

In recent years, with higher worldwide demand for improved quality and corrosion resistance in structural alloys, alternative coatings and coating strategies have been needed. Zinc-based coating alloys, particularly zinc-nickel (Zn-Ni) have been extensively studied due to their technological application in protection against corrosion as an alternative to cadmium (Cd) alloys (Ref 1-3). These alloy coatings are widely applied in the automotive industry, normally at thicknesses of 10 μm (Ref 4). These alloys have also been considered for applications in electrocatalytic water electrolysis (Ref 5), as coatings for steel cord reinforcement of tires (Ref 6), and in the electronics industry (Ref 7). In the Brazilian aeronautical industry, despite their excellent properties as a protective agent, Zn-Ni coatings are still under study and in the development stage. In this industrial segment, good resistance to fatigue is required, which results in another difficulty in the search for alternatives to Cd-based coatings for high-strength steel.

The electrodeposition of Zn-Ni alloys is of the anomalous type due to the preferable deposition of the less noble element Zn (Ref 8). Different hypotheses have been presented to explain this phenomenon, but, despite many studies on the electron deposition process of these coatings, there has been no definitive suggestion as to their mechanism.

H.J.C. Voorwald, I.M. Miguel, and **M.P. Peres,** Fatigue and Aeronautic Materials Research Group, DMT/DME-UNESP/FEG, Av. Ariberto Pereira da Cunha, 333, Guaratinguetá/SP/BR – CEP: 12.516-410; and **M.O.H. Cioffi,** IPOLI-UNESP of Sorocaba, Av. 3 de Março, 511 18087-180 Sorocaba-SP, Brazil. Contact e-mail: voorwald@feg.unesp.br.

The operating conditions of alloy deposition and coating properties were analyzed (Ref 9). The optimum composition of the chloride bath for Zn-Ni electrodeposition was obtained with 11 to 14% Ni. The change in chemical composition of the deposits is also a function of plating bath temperature; for example, Ni content initially increased slowly as the temperature increased from 15 to 60 °C (Ref 3). Another important variable is the thickness of the coverage, and it was observed that values from 5 to 30 μm were used as parameters in the study of characteristics of these alloys in an industrial chloride bath (Ref 10). A range of current densities in the interval 50 to 500 A/m^2 was used to obtain these thicknesses.

Among other things, the thickness of the coatings is directly related to the high tensile residual internal stresses, which result from the presence of Ni in the alloy. Previous studies were carried out with hard Cr electroplating and WC thermal spray coating by HP/HVOF on AISI 4340 high-strength steel (Ref 11-13).

In this study, it was observed that the residual stress decreased with the depth of the coating and increased again at the coating/substrate interface. Bending fatigue tests on specimens with different coatings and coating conditions indicated that the fatigue strength was dependent on the fracture behavior of the substrate and on the hardness and residual stresses at the substrate surface. It was observed also that residual stresses originating from these coatings reduce the fatigue strength of a component (Ref 14).

Due to the negative influence occasioned by corrosion-resistant protective coatings, an effective process like shot peening must be considered to improve the fatigue strength of components and structures (Ref 15). Shot peening proved to be an excellent alternative in increasing the fatigue strength of hard Cr electroplated AISI 4340 steel (Ref 16). Shot peening pushes the crack-initiation site beneath the surface in most medium-cycle and high-cycle cases due to the induced com-

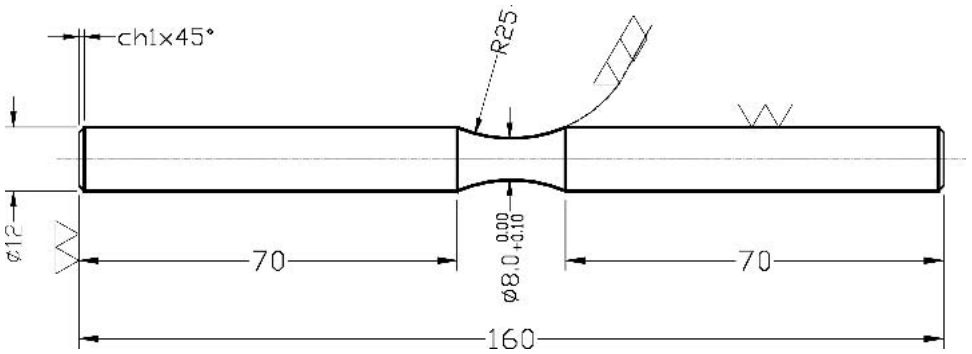

Fig. 1 Rotating bending fatigue test specimen

pressive residual stress field. Rotating bending fatigue data of AISI 4340 steel with 53 HRC hardness indicate that the cracks in shot-peened and non-shot-peened specimens originated at the surface. Some correlation between gain in fatigue strength and crack initiation below the surface was demonstrated (Ref 17).

A series of effects such as structure change within the surface layer, the formation of a residual stress field, and the change of surface roughness have great influence on the fatigue strength of machine parts (Ref 18, 19). Compressive residual stresses induced by machining processes are also responsible for the improvement in the fatigue resistance of AISI 4340 steel (Ref 20).

In the case of aeronautical applications, protection against corrosion must be combined with superior fatigue resistance. The aim of this study was to analyze the effects on AISI 4340 steel with an electroplated Zn-Ni coating on AISI 4340 steel in rotating bending fatigue and to compare these results with those obtained by Cd electroplating. Fracture planes of the fatigue specimens were examined using scanning electron microscopy (SEM) to identify the crack initiation points. Optical metallography (OM) was used to investigate the existence of the uniform coating coverage of the substrates.

Studies of the resistance against corrosion were carried out using salt-spray tests according to ASTM standard B 117. The residual stresses promoted by machining and the electroplating process were obtained and were compared with the base alloy. Residual stresses were determined by x-ray diffraction (Ref 21). The accuracy of the stress measurements was $\Delta\sigma = \pm 20$ MPa. To obtain the stress distribution by depth, the layers of the specimens were removed by electrolytic polishing with a nonacid solution.

2. Experimental Procedure

AISI 4340 steel, widely applied in aircraft components, where strength and toughness are fundamental design requirements, was used as the base alloy in this study. The chemical composition of the steel is in accordance with the required standards.

Rotating bending fatigue test specimens were machined from hot-rolled, quenched-and-tempered bars. Fatigue-test specimens were quenched at temperatures between 815 and 845 °C, placed into oil at 20 °C, and then tempered at 520 ± 5 °C for 2 h. Mechanical properties of the steel after the heat treatment were: Rockwell hardness (38-42 HRC), yield strength (1118 MPa), and ultimate tensile strength (1210 MPa). After final preparation, specimens were subjected to a stress relief heat treatment at 190 °C for 4 h with posterior cooling in still air to reduce the residual stresses induced by machining.

Table 1 Zn-Ni control parameters

Parameters	2-6 μm	8-12 μm	15-21 μm
Process	Hook	Hook	Rotate drum
Zn, %	85-88	91-95	86-90
Ni, %	12-15	5-9	10-14
Bath characteristics			
Zn, g/L	8.0-9.5	7.0-9.0	7.0-10.0
Ni, g/L	1.8-2.2	1.0-1.5	2.0-2.5
Sodium hydroxide, g/L	115-125	120-150	135-145
Sodium carbonate, g/L	0	30-70	0
Maintenance solution, mL/L	22-26	20	25-30
Brightener, mL/L	1.1-1.3	1.0	5.0
Bath temperature, °C	24-28	25-29	25-30
Agitation velocity in bath, m/min	4-6	3-6	…
Cathode current density, A/dm^2	1.0-3.0	1.0-5.0	0.5-1.5
Anode current density, A/dm^2	1.0-2.0	5.0-7.0	0.75-2.00
Deposition velocity, μm/min	0.21	…	…
Conversion coating	Yellow chromating	Yellow chromating	Yellow chromating

Specimens were machined according to the specifications and dimensions illustrated in Fig. 1. After machining, the specimens were polished with 600-grit papers and were inspected dimensionally and by magnetic particle inspection. Average superficial roughness in the reduced section of the specimens was $R_a \approx 2.75$ μm, with a standard deviation equal to 0.89 μm.

2.1 Cd and Zn-Ni Alloy Electroplating

Cadmium electroplating was carried out according to the EMBRAER NE-40-010 standard:

- Specimens were submitted to previous treatment in steam to remove possible residues of solvent
- Chemical degrease treatment (2-5 min), (15-30 s)

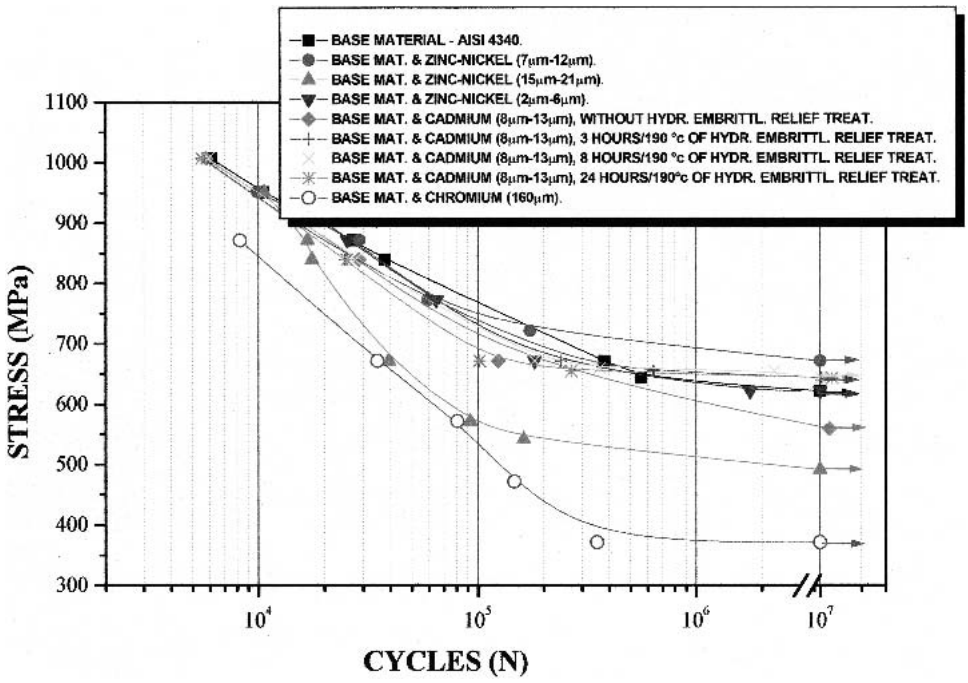

Fig. 2 Rotating bending fatigue test. Base alloy, Zn-Ni alloys, and coatings electroplated with Cd and Cr

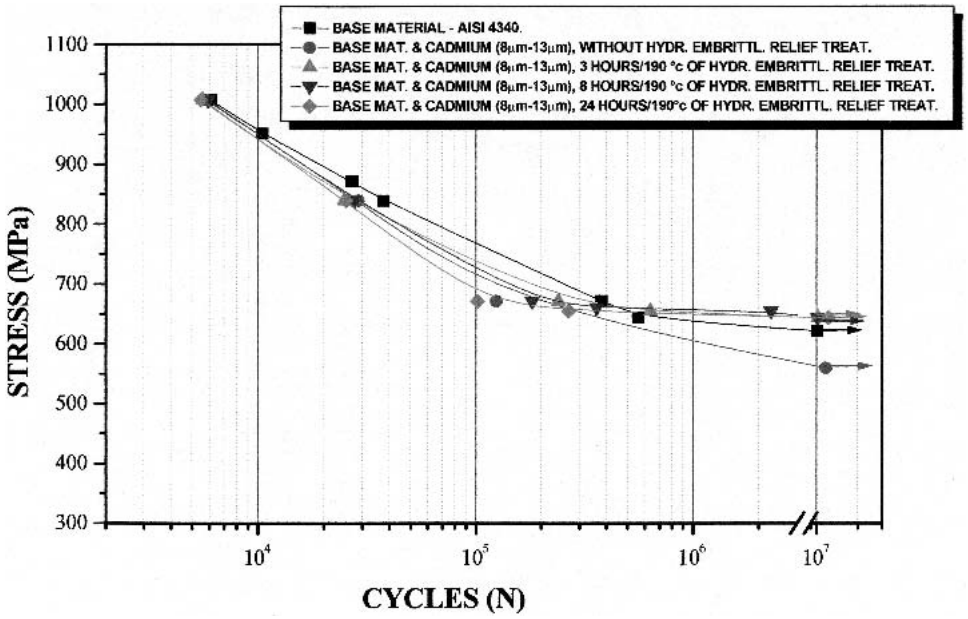

Fig. 3 Rotating bending fatigue test. Base alloy and Cd-electroplated coatings

- Electrolytic degrease (2-5 min), followed by continuous water washing (25-30 s) to clean oils, grease, and other impurities
- Deoxidation (30-60 s), followed by continuous water washing
- Alkali sodium cyanide solution treatment (15-30 s)

The Cd electroplating was carried out using the rotating-drum process for 1 to 10 min to produce coating thicknesses in the range 8 to 13 μm. Parameters used in this process were: Cd salt solution, 20 to 30 g/L; sodium cyanide solution, 90 to 200 g/L; sodium hydroxide solution 10 to 20 g/L; a Cn-to-Cd ratio equal to 4:1 to 6:1; ambient conditions; continuous current between 1 and 5 A/dm^2; voltage anode/cathode, 1 to 4 V; and electrodeposition velocity between 0.2 and 1.5 μm/min. Once bath deposition was completed, the specimens were treated with a sodium cyanide solution for 15 to 30 s, followed by continuous water washing and drying in hot air for 2 to 4 min. The last step in the Cd electrodeposition process was dehydrogenation by heat treatment to avoid the diffusion of hydrogen in the substrate.

The Zn-Ni electroplating was carried out according to the plating-control parameters shown in Table 1. Prior to the deposition, pieces were submitted to pretreatment: alkaline clean-

Table 2 Number of cycles to failure for AISI 4340 steel

σ, MPa	Base alloy			Base alloy + Cd			Base alloy + Cd 190 °C/3 h			Base alloy + Cd 190 °C/8 h			Base alloy + Cd 190 °C/24 h		
	$\overline{N}$	SD	SD $\overline{\gamma}$, %	$\overline{N}$	SD	SD $\overline{\gamma}$, %	$\overline{N}$	SD	SD $\overline{\gamma}$, %	$\overline{N}$	SD	SD $\overline{\gamma}$, %	$\overline{N}$	SD	SD $\overline{\gamma}$, %
1006	6,060	1,932	31.9	5,820	1,450	24.9	5,600	294	5.3	5,875	1,427	24.3	5,533	451	8.2
838	37,729	18,203	48.2	28,783	9,699	33.7	24,867	6,156	24.8	27,720	7,904	28.5	25,400	6,338	25.0
671	488,517	372,223	76.2	124,200	26,850	21.6	240,475	96,692	40.2	182,275	70,189	38.5	101,633	54,360	53.5
654	…	…	…	…	…	…	637,950	99,631	15.6	2,284,225	2,219,436	97.2	268,167	90,043	33.6

ing, acid pickling, and continuous distilled water rinsing. After plating, the specimens were once again rinsed and dried and were subjected to hydrogen-embrittlement relief treatment at 190 °C for 24 h.

2.2 Rotating Bending Fatigue Tests

Rotating bending fatigue tests were performed using a sinusoidal loading at a frequency of 50 Hz and a stress ratio (R) equal to –1.0 in air at room temperature. These tests designate fatigue strength as a complete fracture of the specimens or 10^7 load cycles, whichever occurs first. Nine groups of fatigue specimens were prepared to obtain *S-N* curves for rotating bending fatigue tests:

- 19 smooth specimens of base alloy
- 9 specimens of electroplated Zn-Ni, with thicknesses between 7 and 12 μm
- 10 specimens of electroplated Zn-Ni, with thicknesses between 15 and 21 μm
- 9 specimens of electroplated Zn-Ni, with thicknesses between 2 and 6 μm
- 17 specimens of electroplated Cd, with thicknesses between 8 and 13 μm, heat-treated at 190 °C for 24 h
- 19 specimens of electroplated Cd, with thicknesses between 8 and 13 μm, heat-treated at 190 °C for 8 h
- 17 specimens of electroplated Cd, with thicknesses between 8 and 13 μm, heat-treated at 190 °C for 3 h
- 16 specimens of electroplated Cd, with thicknesses between 8 and 13 μm
- 16 specimens of electroplated Cr, with thicknesses of 100 μm

2.3 Salt-Spray Tests

The performance of Zn-Ni alloy coatings was evaluated with respect to chemical corrosion resistance in a specific environment. The test panels were prepared from normalized AISI 4340 steel, 254 mm in length by 76 mm in width by 1 mm in thickness, with a surface roughness $R_a \approx 0.2$ μm and electroplated to 100 μm thickness with the Zn-Ni alloy.

Experiments were carried out in accordance to ASTM standard B 117 in a 5 wt.% NaCl solution with a pH of 6.5 to 7.2 at 35 °C. Specimens were supported at 20° from the vertical. Tests results were analyzed by visual inspection of the area exposed to the environment.

2.4 Adhesion Tests

The performance of Zn-Ni alloy coatings was also verified with respect to adhesion using specimens prepared from normalized AISI 4340 steel that were 90 mm in length by 25 mm in width with a surface roughness $R_a \approx 0.2$ μm. The specimens were divided into three groups in the following conditions:

- 6 specimens of electroplated Zn-Ni alloy, with thickness between 8 and 12 μm
- 6 specimens of electroplated Zn-Ni alloy, with thickness between 15 and 21 μm
- 6 specimens of electroplated Zn-Ni alloy, with thickness between 2 and 6 μm

The adhesion tests were conducted according to the ASTM E 290 and SAE-AMS 2417E standards.

2.5 Residual Stress Analysis

Residual stress analyses were conduced using a portable x-ray apparatus with an air-cooled double-anode x-ray tube. It was provided with a stress measurement unit and focusing camera for phase analysis. A description of the equipment and the methodology applied during the tests is described by Monin et al. (Ref 22). The specimens used in these tests had the same specifications adopted for the fatigue tests and are shown in Fig. 1. Measurements were carried out on the base alloy and the Zn-Ni electroplated base alloy at the interface between the substrate and coatings and in regions within the substrate.

2.6 Fracture Surface Analysis and Metallographic Characterization

Fracture surface analysis was carried out on rotating bending fatigue test specimens by SEM. Metallographic analysis was carried out by OM.

Images were used to identify the extent of coating coverage of the substrates and to investigate the performance of the coatings with respect to their adherence properties. The thicknesses of the coatings were measured and compared to verify their relationship with fatigue behavior. Metallographic analysis was carried out on specimens sectioned in the transverse direction, mounted in acrylic resin, and polished using 80-grit to 1000-grit graduated waterproof abrasive papers and 99.98% alumina suspension.

3. Results and Discussion

3.1 Fatigue Tests

Figure 2 shows *S-N* curves for the rotating bending fatigue tests of the base alloy, the hard Cr coating, the Cd coating, and the Zn-Ni coating. The influence of the hydrogen-

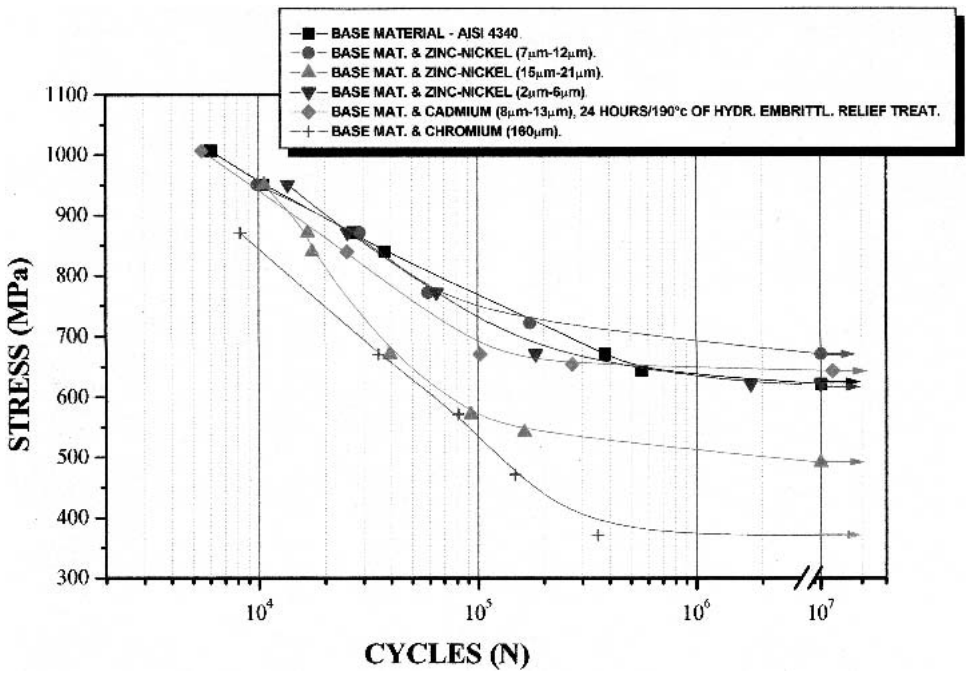

Fig. 4 Rotating bending fatigue test. Base alloy, Cd-electroplated coating (24 h and 190 °C), and Zn-Ni alloy coatings

embrittlement relief heat-treatment time on AISI 4340 steel fatigue strength is shown in Fig. 3.

Experimental data for the base alloy in Fig. 2 is used in this work as a reference for comparison with the fatigue strength of AISI 4340 steel electroplated with Cd and Zn-Ni. It is possible to observe from Fig. 2 a significant reduction in the fatigue life for the Cr-electroplated specimens. To understand the influence of Cd and the heat treatment times at 190 °C on the *S-N* curves, Fig. 3 should be analyzed. The importance of the heat treatment after Cd electroplating in avoiding hydrogen embrittlement is clearly indicated in Fig. 3. The *S-N* curve for the specimens tested after Cd electroplating, without post heat treatment, shows a decrease in fatigue strength compared with the base alloy for the low and high cycles.

The reduction in the number of cycles to failure associated with Cd electroplating without post heat treatment is presented in Table 2. From Fig. 3, it is also possible to observe that for a number of cycles $>10^5$, the fatigue strength of the Cd-electroplated specimens with post heat treatment increased in comparison to those without heat treatment. Table 2 shows a decrease in fatigue strength for Cd-electroplated and post-heat-treated AISI 4340 steel at 190 °C for 24 h in comparison to the rotating bending fatigue test results at 3 and 8 h. This may be due to Cd diffusion in the base alloy resulting in a lower fatigue life of the specimen. Table 2 shows a decrease in the fatigue strength for AISI 4340. Considering the scatter in the fatigue tests, little influence of heat treatment times in the fatigue strength is observed. For low-cycle fatigue, the influence of Cd electroplating is not clearly observed.

Figure 4 shows the effect of Zn-Ni-electroplated coatings with thicknesses of 2 to 6 μm, 7 to 12 μm, and 15 to 21 μm on the fatigue strength of AISI 4340 steel. As a comparison, *S-N* curves for Cr-electroplated specimens (160 μm coating thickness), and specimens Cd electroplated and heat treated at 190 °C for 24 h are also shown.

Work by Nascimento et al. (Ref 11) showed the influence of microcrack density on the fatigue strength of AISI 4340 steel

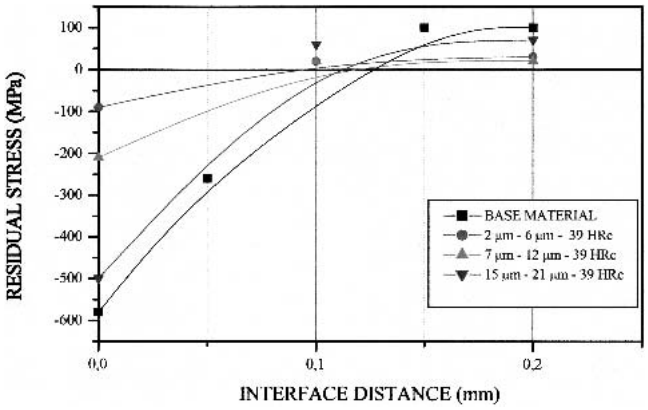

Fig. 5 Residual stress measurement tests

Table 3 Residual stress analysis

	Residual stress, MPa		
Specimens	***h* = 0.0 mm**	***h* = 0.1 mm**	***h* = 0.2 mm**
Base alloy	−580	−260	+100
2-6 μm	−90	+20	+30
7-12 μm	−210	+20	+20
15-21 μm	−500	+60	+70

Note: Residual stress of steel without machining: 52 to 97 MPa; h, access depth of x-ray.

with Cr-electroplated coatings. In general, the fatigue strength was reduced due to the high tensile residual internal stress, microcrack density, and high adhesion strength at the coating/substrate interface.

To understand the effect of Zn-Ni-electroplated coatings on the *S-N* curves for AISI 4340 steel, Fig. 5 and Table 3 should be considered. From Fig. 5 (i.e., the residual stress at the sub-

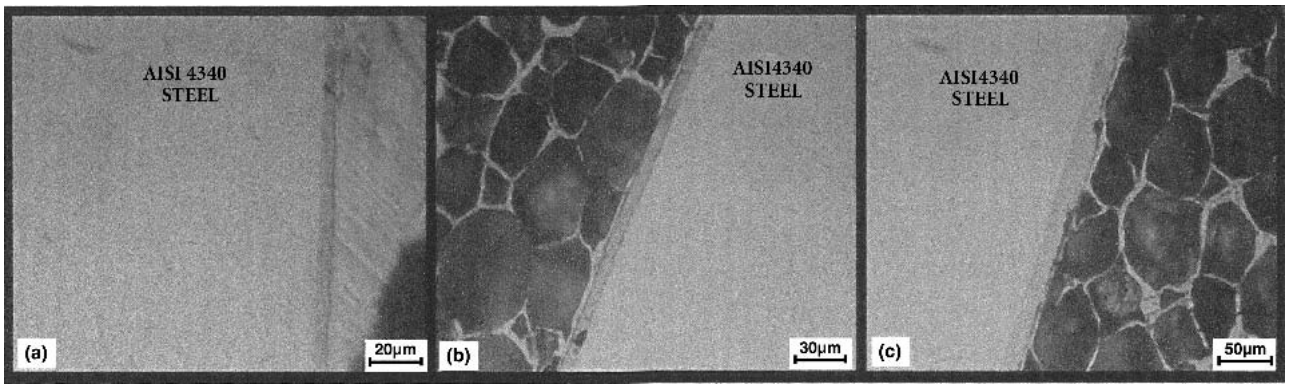

Fig. 6 OM of thicknesses and homogeneity of Zn-Ni layers. (a) 2 to 6 μm. (b) 7 to 12 μm. (c) 15 to 21 μm

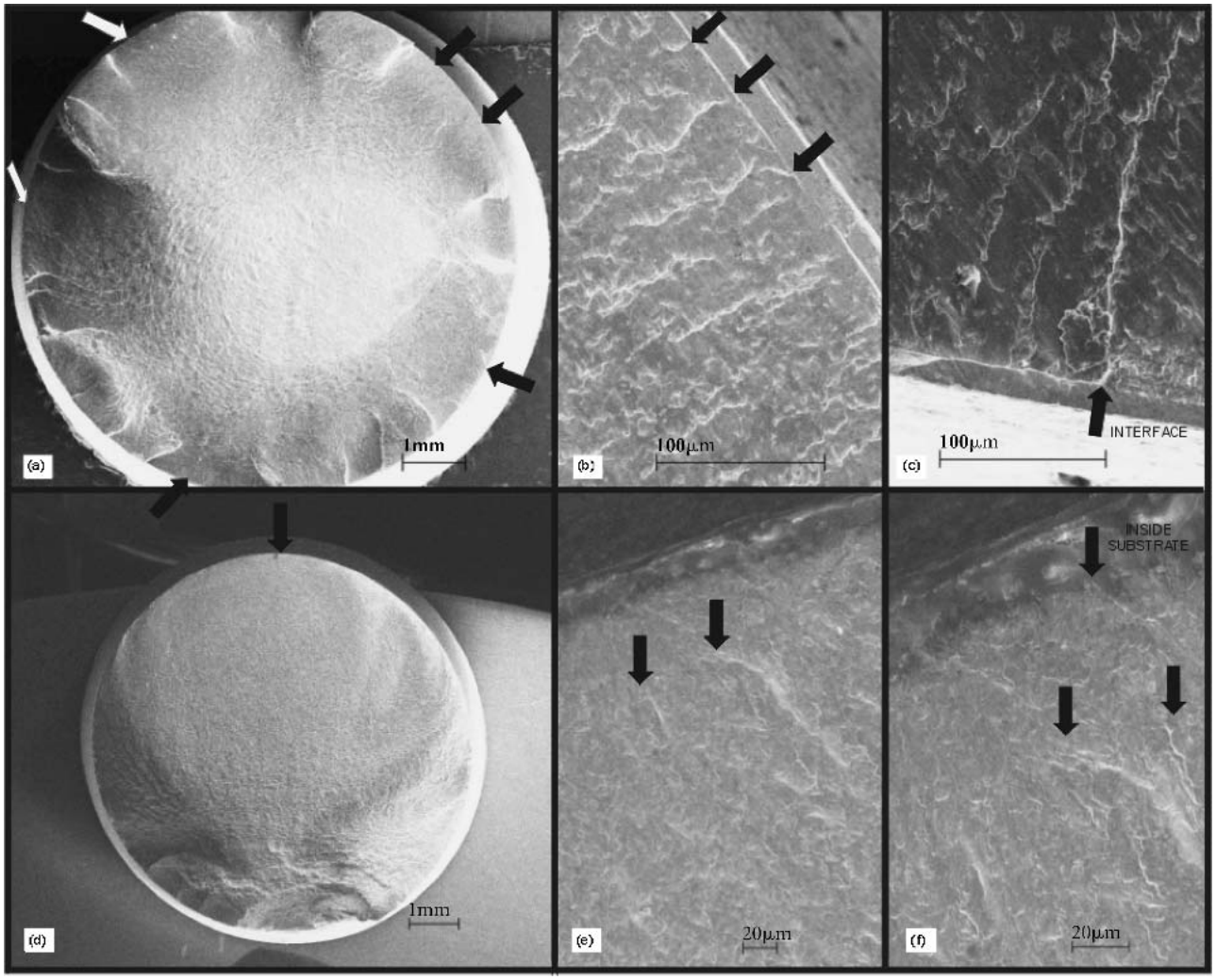

Fig. 7 SEM image of AISI 4340 Zn-Ni alloy coatings: thicknesses, 15 to 21 μm

strate/coating interface and inside base alloy), the compressive residual stress at the interface decreases with the decrease in the coating thickness. The maximum compressive residual stress at the interface is obtained for the base alloy. It is interesting to observe the variation in the residual stress as the distance from the interface increases. After 0.1 mm, Zn-Ni-electroplated specimens with thicknesses in the range of 7 to 12 μm and 15 of 21 μm showed tensile residual stresses of 20 and 60 MPa, respectively. For the base alloy and the Zn-Ni-electroplated coating in the range of 2 to 6 μm, Table 3 shows that at 0.1 mm from the interface the residual stresses are −260 and 20 MPa, respectively.

At 0.2 mm from the interface, all conditions show a tensile residual stress in the range of 20 to 100 MPa. It is interesting to observe that for the Zn-Ni-electroplated coating that is 15 to 21 μm in thickness, the variation in residual stress goes from

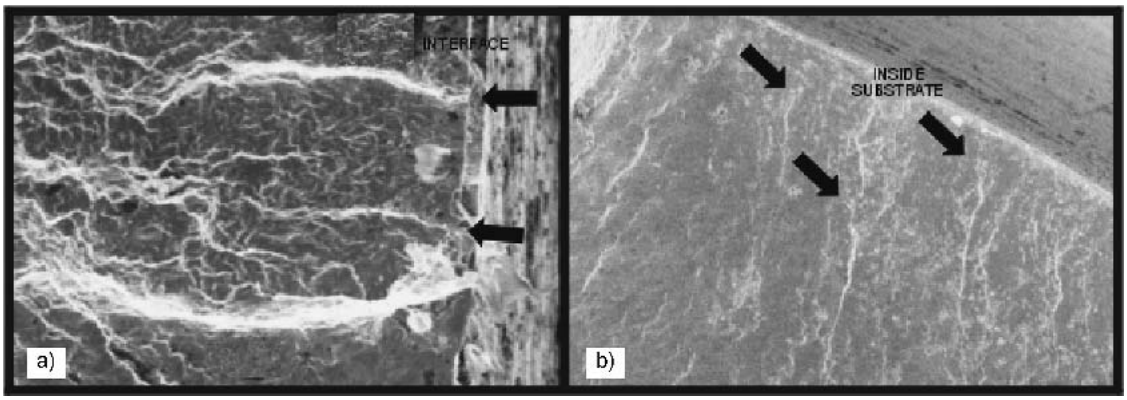

Fig. 8 SEM image of AISI 4340 electroplated with Zn-Ni alloys with coatings of thicknesses of 7 to 12 μm

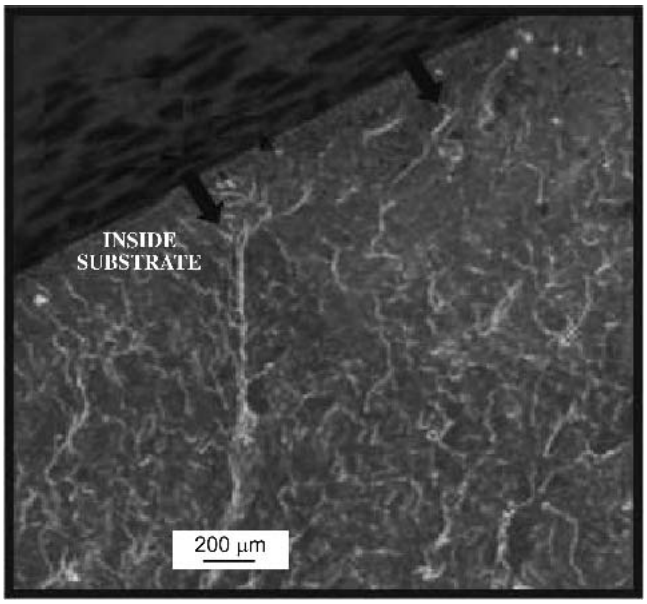

Fig. 9 SEM image of AISI 4340 Zn-Ni-electroplated alloy coatings with thicknesses of 2 to 6 μm

500 MPa compressive at the interface to 60 MPa tensile at 0.1 mm from that point. Comparison between residual stresses at 0.1 and 0.2 mm from the interface indicate, except for the base alloy, almost the same results for the Zn-Ni-electroplated coatings.

Figure 4 shows that a decrease in the rotating bending fatigue strength occurred in AISI 4340 Zn-Ni-electroplated specimens with thicknesses in the range 15 to 21 μm. In the case of coatings that were 7 to 12 μm thick, the experimental results were close to those obtained for the base alloy.

It is well known that a delay in fatigue crack nucleation and propagation results from the presence of a compressive residual stress field, which, consequently, increases the fatigue strength. Table 3 shows that the compressive residual stresses at the interface for coating thicknesses of 2 to 6 μm, 7 to 12 μm, and 15 to 21 μm were 90, 210, and 500 MPa, respectively. To understand the behavior of the *S-N* curves represented in Fig. 4, residual stresses at 0.1 mm from the coating/substrate interface must be considered. The highest residual stress was obtained for the Zn-Ni-electroplated coating with a thickness of 15 to 21 μm, compared to those of 2 to 6 and 7 to 12 μm.

Figure 5 shows the residual stress behavior with a compressive stress at the interface and a tensile stress 0.1 mm from that point for the base alloy and the three Zn-Ni-electroplated coating thicknesses studied.

Figure 6(a) shows an OM image of the Zn-Ni-electroplated coating, 2 to 6 μm thick, at a magnification of 1000×. It is possible to verify that the coating layer is uniform and that there are no signs of coating detachment from the substrate. Figure 6(b) and (c) show images from specimen coating thicknesses of 7 to 12 μm and 15 to 21 μm, respectively. Coating homogeneity and strong adhesion with the substrate are observed.

Figure 7(a) to (c) shows the fracture surfaces of a rotating bending fatigue specimen tested at 951 MPa that fractured after 10,600 cycles. The electroplated Zn-Ni coating thickness was in the range 15 to 21 μm. Figure 7(a) shows the general fracture surface with several crack-initiation sites around the specimen periphery. Figure 7(b) shows a fatigue crack nucleation site at the coating/substrate interface. In Fig. 7(c), fatigue crack nucleation occurs at the interface with propagation occurring inside the substrate. Figure 7(d) to (f) are associated with a fatigue specimen tested at 571 MPa with a number of cycles to a fracture equal to 83,600 cycles.

Figure 7(e) and (f) show fatigue crack initiation, which is associated with the variation in residual stresses, inside the substrate of 500 MPa compressive at the interface and 600 MPa tensile at 0.1 mm from this region. Figure 8(a) and (b) show the fracture surface from the base alloy for a Zn-Ni-electroplated specimen with a thickness in the range of 7 to 12 μm that was tested at 951 MPa ($N = 9500$ cycles). Fatigue crack initiation occurs at the specimen surface, inside the coating at the interface of the coating and substrate.

Figure 9 shows the fracture surface of the AISI 4340 steel with Zn-Ni-electroplated coating with thickness between 2 and 6 μm tested at 771 MPa, which fractured after 74,600 cycles. In this case, crack origins were observed inside the substrate.

3.2 Salt-Spray Tests

Figure 10 shows the results of the salt-spray tests carried out on the Zn-Ni-electroplated coatings, performed in a qualitative way by visual inspection of the specimens after exposure to the environment. Coatings with thicknesses between 15 and 21 μm (Fig. 10a) and 7 and 12 μm (Fig. 10b) guarantee complete corrosion protection. However, for the coating with thicknesses

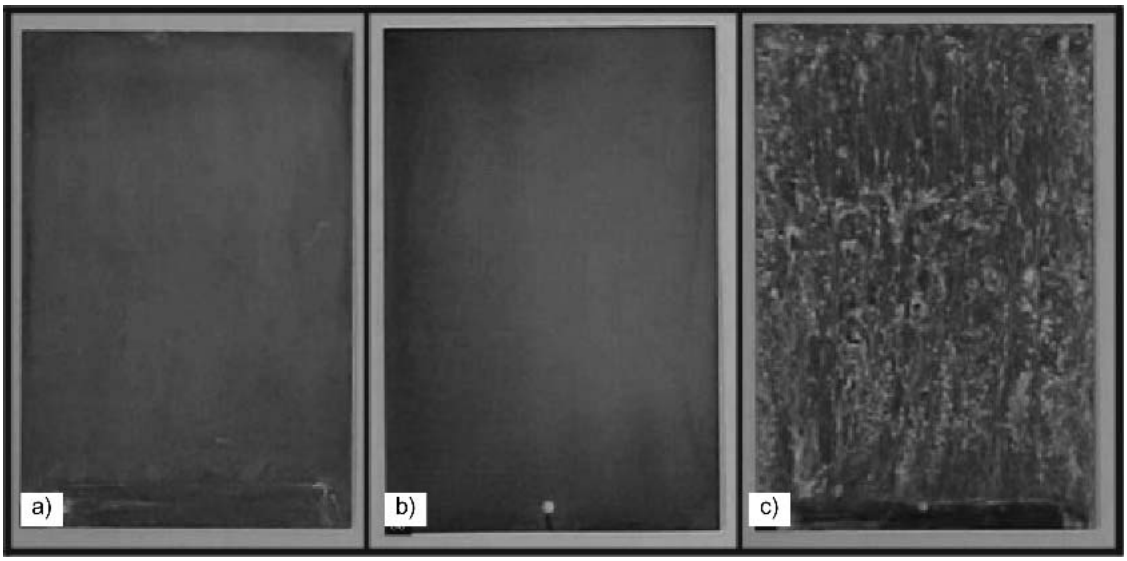

Fig. 10 Salt-spray tests of AISI 4340 Zn-Ni-electroplated alloy coatings. (a) 15 to 21 μm. (b) 7 to 12 μm. (c) 2 to 6 μm

Fig. 11 Adhesion tests of AISI 4340 Zn-Ni-electroplated alloy coatings. (a) 2 to 6 μm. (b) 712 μm. (c) 15 to 21 μm

in the range of 2 to 6 μm (Fig. 10c), the completed salt-spray test results showed the exposed areas to be completely corroded.

3.3 Adhesion Tests

Figure 11 shows images obtained from adhesion tests for the Zn-Ni-electroplated coatings. Figure 11(a) shows a specimen with a coating thickness of 2 to 6 μm, Fig. 11(b) shows a specimen with a coating thickness of 7 to 12 μm, and Fig. 11(c) shows a specimen with a coating thickness of 15 to 21 μm. In these figures, the separation of the coating from the base metal after they were bent at room temperature through an angle of 180° around a diameter equal to the thickness of the specimen was not observed.

4. Conclusions

- Rotating bending fatigue tests indicate differences between specimens not exposed and those exposed to temperature/time to avoid hydrogen embrittlement, for a number of cycles $>10^5$; in the case of AISI 4340 steel Cd electroplated.
- For low-cycle fatigue, differences in fatigue strength for specimens exposed at 190 °C for 2, 8, and 24 h were not observed. In high-cycle fatigue, some influence was detected, indicating better results for lower treatment times.
- The reduction in the AISI 4340 steel rotating bending fatigue strength resulted from Zn-Ni-electroplated coating in the thickness interval of 15 to 21 μm. In the case of a coating thickness of 7 to 12 μm, experimental data indicated almost the same behavior with respect to the fatigue strength as that showed by the AISI 4340 Cd-electroplated steel with a coating thickness of 8 to 13 μm.
- With respect to the adhesion tests, Zn-Ni-electroplated coating thicknesses passed according to ASTM E 290 and SAE-AMS 2417E standards.
- Salt-spray tests showed that complete surface corrosion occurred for the Zn-Ni-electroplated coating in the thickness range of 2 to 6 μm, while the coatings in thickness ranges of 7 to 12 μm and 15 to 21 μm passed according to the ASTM B 117 standard.

Acknowledgments

The authors are grateful for the support of this research by CAPES, ELEB/EMBRAER, and FAENQUIL/DEMAR.

References

1. I.M. Miguel, C.E.A. Silva, M.P. Peres, and H.J.C. Voorwald, Study of Influence of Zinc-Nickel and Cadmium Electroplated Coatings on Fatigue Strength of Aeronautical Steels, *Fatigue,* 2002, p 15-23

2. S.B. Silva, L.H. Mascaro, S.A.S. Machado and L.A. Avaca, "Análise da Composição de Ligas de Zn-Ni Depositadas sobre Diferentes Materiais," presented at EBRATS 94, 1994, p 15-23
3. G.F. Hsu, Zinc-Nickel Alloy Plating: An Alternative to Cadmium, *Plat. Surf. Finish.,* Vol 71 (No. 4), 1984, p 52-55
4. A.M. Alfantazi and U. Erb, Corrosion Properties of Pulse-Plated Zinc-Nickel Alloy Coatings, *Corros. Eng.,* 1996, p 880-888
5. M.J. Giz, S.A. Machado, L.A. Avaca, and E.R. Gonzalez, High Area Ni-Zn and Ni-Co Codeposits as Hydrogen Electrodes in Alkaline Solutions, *J. Appl. Electrochem.,* Vol 22, 1992, p 973-977
6. J. Giridhar and W.J. Ooij, *Surf. Coat. Technol.,* Vol 53, 1992, p 35
7. R.G. Baker and C.A. Holden, Zinc-Nickel Alloy Electrodeposits: Rack Plating, *Plat. Surf. Finish.,* Vol 72 (No. 3), 1985, p 54-57
8. D.E. Hall, Electrodeposits Zinc-Nickel Ally Coatings: A Review, *Plat. Surf. Finish.,* Vol 70, 1983, p 59-65
9. T. Zhenmi, Z. Jingshuang, A. Maozhong, Y. Zhelong, and Z. Zhijun, "Electrodeposition of Zinc-Nickel Alloys from Chloride Bath with High Throwing Power," presented at EBRATS 94, 1994, p 35-41
10. G. Barceló, E. Garcia, M. Sarret, and C. Müller, Characterization of Zinc-Nickel Alloys Obtained from an Industrial Chloride Bath, *J. Appl. Electrochem.,* Vol 28, 1998, p 1113-1120
11. M.P. Nascimento, R.C. Souza, I.M. Miguel, W.L. Pigatin, and H.J.C. Voorwald, Effects of Tungsten Carbide Thermal Spray Coating by HP/HVOF and Hard Chromium Electroplating on AISI 4340 High Strength Steel, *Surf. Coat. Technol.,* Vol 138, 2001, p 113-124
12. R.C. Souza, M.P. Nascimento, H.J.C. Voorwald, and W.L. Pigatin, The Effect of WC-17Co Thermal Spray Coating by HP/HVOF and Hard Chromium Electroplating on the Fatigue Life and Abrasive Wear Resistance of AISI 4340 High Strength Steel, *J. Mech. Behav. Mater.,* Vol 12, 2001, p 121-140
13. R.C. Souza, M.P. Nascimento, H.J.C. Voorwald, and W.L. Pigatin, The Effect of WC-10Co-4Cr and CrC-25NiCr HVOF Coatings on the Fatigue Strength of AISI 4340 Steel, *Fatigue,* 2002, p 2453-2460
14. S. Hotta, Y. Itou, K. Saruki, and T. Arai, *Surf. Coat. Technol.,* Vol 96, 1997, p 148
15. S.P. Wang, Y.J. Li, M. Yao, and R. Wang, Compressive Residual Stress Introduced by Shot Peening, *J. Mater. Proc. Technol.,* 1998, p 64-73
16. M.P. Nascimento, R.C. Souza, I.M. Miguel, W.L. Pigatin, and H.J.C. Voorwald, Effects of Surface Treatments on the Fatigue Strength of AISI 4340 Aeronautical Steel, *Int. J. Fatigue,* Vol 23, 2001, p 607-618
17. M.A.S. Torres and H.J.C. Voorwald, An Evaluation of Shot Peening, Residual Stress and Stress Relaxation on the Fatigue Life of AISI 4340 Steel, *Int. J. Fatigue,* Vol 24, 2002, p 877-886
18. P. Starker, H. Wohlfahrt, and E. Macherauch, Fatigue Fract. Eng. Mater. Struct., Vol 1, 1979, p 319
19. S.M. Kudva and D.J. Duquette, Effect of Surface Residual Stress on the Fretting Fatigue of 4340 Steel, *Residual Stress Effects in Fatigue,* STP 776, ASTM, 1982, p 195-203
20. Y. Matsumoto, D. Magda, D.W. Hoeppner, and T.Y. Kim, *J. Eng. Indust.,* Vol 113, 1991, p 54
21. T. Gurova, Study of the Residual Stress State During Plastic Deformation Under Uniaxial Tension in a 5.0 Cr and 0.5 Mo Steel, *Sci. Mater.,* Vol 36 (No. 9), 1997, p 1031-1035
22. V. Monin, J.R. Teodosio, and T. Gurova, A Portable X-Ray Apparatus for Both Stress Measurement and Phase Analysis Under Field Conditions, *Adv. X-Ray Anal.,* Vol 43, 2000, p 66-71